Wave generation by flap-type wavemaker in circle arc numerical wave tanks

Qiaosha Wang, Minghai Li*

Institute of Systems Engineering, China Academy of Engineering Physics, Mianyang 621900, China.

*Corresponding author e-mail: Limh@caep.cn

Abstract. A circle arc numerical wave tank for wave generation in a geotechnical centrifuge is presented in this paper. Compared with traditional straight wave tank, the use of the circle arc numerical wave tank can minimize the error due to the radial gravity field which produced by the centrifugal acceleration. A variety of cases generated by flap-type wavemakers in intermediate and deep waters are simulated in the circle arc numerical wave tanks and the accuracy of the numerical results are verified by a comparison with the numerical results in traditional straight wave tanks and the results of wavemaker theory. The results show that the wavemaker theory produced by Ursell can be used both in traditional straight numerical wave tanks but also in circle arc numerical wave tanks. The slight discrepancy of the results between the circle arc wave tanks and the traditional straight wave tanks can be attributed to the nonlinear effect caused by the circle arc. However, the discrepancy is insignificant which can be neglected for a circle arc wave tank with a relative long radius.

1. Introduction

With the rapid development of marine science and technology, the ocean engineering services in more severe environment and the design precision of ocean engineering improves constantly; the complexity of the involved problems improves constantly. The limitations and restrictions of the conventional physical experiments are increasingly prominent. The ocean engineering tends to be massive and the prototype observation or full-scale experiments tends to be rather costly. Therefore, small scale models are used in most of conventional physical experiments. However, the stresses and self-weight in prototype cannot be simulated properly by small scale models and the stress-stain behaviour of most models are to be non-linear. Therefore, the behaviour of a scaled-down model may not represent the behaviour to its prototype. And with the centrifuge, self-weight stresses and gravity-depended processes can be related to the full-scale prototype situation using well established scaling laws [1]. Hence, centrifuge experiments are frequently used in the laboratory to study the actual prototype's behaviour. The generation and propagation of gravity surface waves in a drum centrifuge, with application to seabed mechanics, are discussed by Sekiguchi and Phillips [2]. After that, the generation and propagation of waves in geo-centrifuge are discussed, with application to wave-induced liquefaction of sand beds [3-5]. And then several researchers developed centrifuge experiments to the study of submarine slide [6-9].

At the present centrifuge experiments are only used for the geotechnical engineering, however, the water wave problems as the basic of marine engineering can not be reproduced properly in centrifuge yet. And but few people study on the water wave problems in Ng force field. The rely on the wave tanks is likely the primary cause, such as wave generation [10-14], wave reflection [15] and the interaction between waves and slopes [16]. And wave tanks are too huge for centrifuge equipment at the present such as the wave tanks created by Sekiguchi [3] and Sassa [4-5] which the wave tank length is only one wave length and can not meet the requirements of most of the marine engineering experiments. Therefore, the creating of wave tanks properly in a centrifuge is the primary problem. And the length of the wave tank in a centrifuge should be much longer than most of current centrifuge modeling.

At the present the geotechnical centrifuge basket always is a cuboid with a similar width, length and height which has a rectangle cross section in radial gravity field. However, wave tanks always have a much longer length and a shorter width and height. Therefore a circle arc cross section should be used in radial gravity field for minimise the errors in centrifuge modeling (the details about the reason is described in section 2). And in this paper, wave generation in a circle arc numerical wave tank is presented. To verify the effectiveness of wave generation in the circle arc numerical wave tank, the results are compared with the results generated in the straight numerical wave tanks. A dynamic mesh technology is used to simulate the wavemaker's flapper which simulation the real physics of wave generation phenomenon. And the unsteady, two dimensional Reynolds Averaging Navier-Stokes equations are solved in conjunction with the RNG k-ε model for treating the turbulence and the volume-of-fluid (VOF) method [17] for treating the free surface.

2. General theory

Despite the fact that the centrifuge is a very powerful tool for reproducing the behavior of a prototype in a small-scale model, there also are some restrictions and limitations, too. In order to minimize the errors caused by these reasons it is essential to identify and quantify these limitations. A centrifuge is able to provide the N times gravity field. In this paper, the beam centrifuge is considered. A schematic of the beam centrifuge is shown in Fig. 1. When a centrifuge is rotating with an angular velocity of ω_c, the centrifugal acceleration at any radius r can be given by $r\omega_c^2$. Therefore, $Ng=r\omega_c^2$ is defined where N always is defined as model scale in a centrifuge model testing in order to match this centrifuge acceleration to be the same as the prototype. From the function, $Ng=r\omega_c^2$, it can be understood that the gravity field produced by a centrifuge is a radial field. However, the gravity field which provided by the earth is assumed to be vertically downwards or parallel in the context of geotechnical structures.

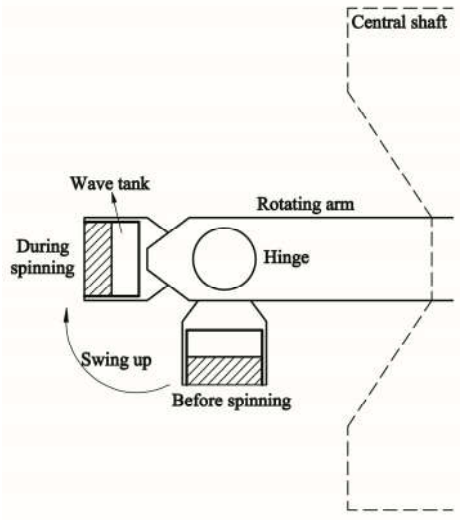

Fig. 1 A schematic of the beam centrifuge. The drawing is not to scale.

Fig. 2 shows the error of the radial gravity field. It can be seen that in the center of the model, for traditional rectangular cross section models, the direction of the acceleration is in the vertical direction, while towards the side of the model the acceleration becomes more inclined. And it can also be seen that the error due to the radial gravity field becomes serious in a longer length model (as shown in Fig. 2 (a)). Therefore, the effect may cause a significant error if testing activity is in the region close to the sides of the model or when the model is much longer which can not be avoided in a wave tank model. However, this problem becomes insignificant in a circle arc model, no matter for a shorter model or for a longer model, as the model is along the circle arc where the direction of the acceleration is always vertical relative to the model (as shown in Fig. 2 (b)).

At the present study, wave generation in a circle arc numerical wave tank is presented for minimizing the errors caused by the radial gravity field. For minimizing the other errors in a centrifuge modeling, such as variations of stress and gravity field with model depth and the Coriolis effects which be not considered in this study, there are various literatures have been presented [1, 9, 18-19].

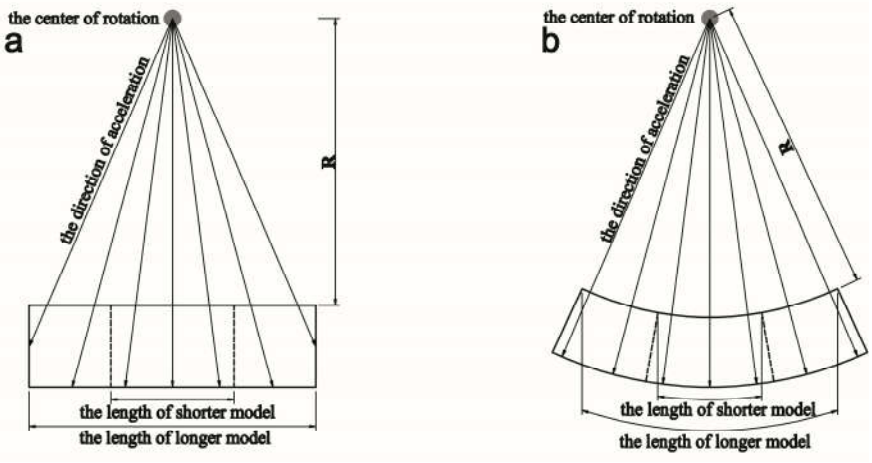

Fig. 2 Error due to radial gravity field

3. Governing equations and boundary conditions

The schematic of the wavemaker mechanisms considered in this study is given in Fig. 3. The domain of the computation are annulus ($\theta \times D$) for circle arc wave tanks and rectangle ($L \times D$) for straight wave tanks with one damping zone at the right end of the tank as shown in the figure. The wavemaker is positioned at the left end of the tank and forced to move according to a prescribed harmonic motion. The flap type wavemakers are considered in this paper which used by other researches such as Ducrozet et al. [20], Anbarsooz et al. [21] and Gyongy et al. [22], not only in numerical wave tanks, but also in physical wave tanks.

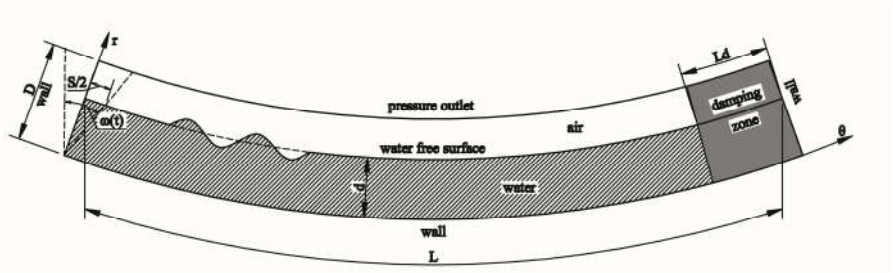

a

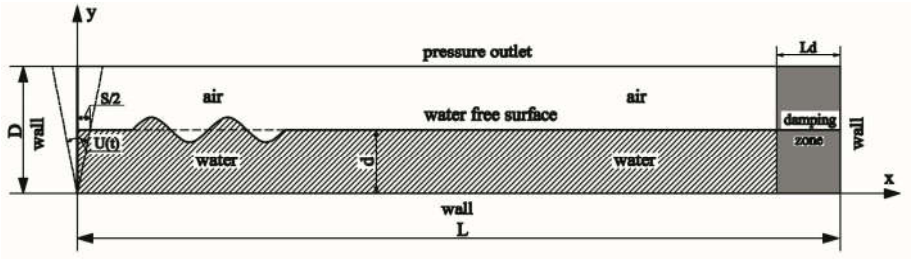

b

Fig. 3 Computational domain and boundary conditions for: (a) circle arc numerical wave tank; and (b) straight numerical wave tank. The drawing is not to scale.

3.1. Governing equations

The governing equations for fluid flow are the Reynolds Averaging Navier-Stokes equations in 2 dimensional, Newtonian and incompressible:

$$\frac{\partial u_i}{\partial x_i} = 0 \tag{1}$$

$$\rho \frac{\partial u_i}{\partial t} + \rho \frac{\partial \left(u_i u_j\right)}{\partial x_j} = -\frac{\partial P}{\partial x_i} + \rho f_i + \frac{\partial}{\partial x_j}\left(\mu \frac{\partial u_i}{\partial x_j} - \rho \overline{u_i' u_j'}\right) \tag{2}$$

where u and u' are the fluctuating and mean velocity components, ρ is the density, P is the pressure, μ is the dynamic viscosity, f_i represents body forces acting on the fluid and $-\rho\overline{u_i' u_j'}$ is Reynolds stresses which must be solved in order to close the Reynolds Averaging Navier-Stokes equations. In this study, the RNG k-ε two equations model is considered for solving the Reynolds stresses and closing the Reynolds Averaging Navier-Stokes equations, which defined as:

$$\rho \frac{\partial k}{\partial t} + \rho \frac{\partial \left(k u_i\right)}{\partial x_i} = \frac{\partial}{\partial x_j}\left[\alpha_k \mu_{eff} \frac{\partial k}{\partial x_j}\right] + G_k - \rho\varepsilon \tag{3}$$

$$\rho \frac{\partial \varepsilon}{\partial t} + \rho \frac{\partial \left(\varepsilon u_i\right)}{\partial x_i} = \frac{\partial}{\partial x_j}\left[\alpha_\varepsilon \mu_{eff} \frac{\partial \varepsilon}{\partial x_j}\right] + C_{1\varepsilon} \frac{\varepsilon}{k} G_k - C_{2\varepsilon}^* \rho \frac{\varepsilon^2}{k} \tag{4}$$

Eq. 3 and 4 are the k and ε transport equations for the turbulence kinetic energy and turbulence dissipation rate respectively.

The water free surface is treated using the VOF method by means of a scale filed (f) defined as:

$$f=\begin{cases}0 & \text{in the gas phase}\\ (0,1) & \text{in the liquid-gas interface}\\ 1 & \text{in the liquid pahse}\end{cases} \tag{5}$$

The scale field propagating according to:

$$\frac{\partial f}{\partial t}+\frac{\partial(u_i f)}{\partial x_i}=0 \tag{6}$$

All equations mentioned above are presented in Cartesian Coordinates. For treating circle arc wave tanks the coordinate (x, y) is defined as:

$$\begin{cases}x=r\cos\theta\\ y=r\sin\theta\end{cases} \tag{7}$$

3.2. Initial and boundary conditions

The initial condition considered in this study is still water. At the left, right and bottom boundaries of the computational domain, the no slip condition for the velocity components are imposed. At the top of the domain, the outlet boundary with atmospheric pressure is used.

For the wave generation, the wavemaker's paddle with a prescribed motion is modeled using the dynamic mesh technology. The position and orientation of the paddle are calculated each time step based on its prescribed motion and corresponding velocity distribution of the paddle is updated accordingly. In this study, the paddle has no translational velocity, but a simple harmonic angular velocity as:

$$\begin{cases}\theta(t)=\frac{t}{2T}\frac{\Delta\theta}{2}\omega\cos(\omega t) & t\le 2T\\ \theta(t)=\frac{\Delta\theta}{2}\omega\cos(\omega t) & t>2T\end{cases} \tag{8}$$

where T is the period, $\Delta\theta$ is the angular span of the flapper motion, ω is the angular wave frequency defined by $2\pi/T$. The stroke of the flapper (S) depends on both the angular span and the still water depth as:

$$S=2d\tan\left(\frac{\Delta\theta}{2}\right) \tag{9}$$

In this study, the motion of the flapper is initiated using a linear time ramp according to Zhao et al. [23]. A duration time of $2T$ for the time ramp is enough to eliminate the initial instabilities.

For the absorption of the wave energy, the damping zone must be modeled. Lin and Liu [24] introduced a friction source term in the momentum equation with an exponential damping law. Hafsia et al. [25] employed the same concept but simplified it. Anbarsooz et al. [21] introduced another method for treating the damping zone. The method is increased viscosity to a high level enough to effectively damp the energy of incident wave. In the present study, one passive absorption zones (see Fig. 3) are modeled in the simulation, at the left end of the computational domain. The method for treating these regions is increased a friction source term in the momentum equation with a linear damping law.

3.3. Numerical method

In this study, the Finite Volume Method (FVM) is used for solving the governing equations in conjunction with the Semi-Implicit Method of Pressure-Linked Equations (SIMPLE) algorithm for solving the problem of Pressure-Velocity Coupling. The second-order upwind scheme is used for the discretization of the momentum, turbulent kinetic energy and turbulent dissipation rate equations and

the pressure staggering option (PRESTO!) scheme is used for the discretization of the pressure equation. The VOF method is used to track the location of the interface which is solved according to the geometric reconstruction schemes.

4. Results and discussions

Wave steepness (H/l, H is the wave height and l is the wave length) is considered no greater than 0.025 and the ratio of $2\pi d/l$ (d is the still water depth) is considered no less than 2.0 in order to avoid the strong nonlinear effect caused by wave steepness and the water depth. The experimental conditions corresponding to these cases are shown in Table 1.

Table 1. Wavemaker conditions

Number	T (s)	H (cm)	S (cm)	H/l	2πd/l
1	0.9	2	1.39	0.0158	3.48
2	0.9	2.5	1.74	0.0198	3.48
3	0.9	3	2.08	0.0238	3.48
4	1	2	1.52	0.0129	2.84
5	1	2.5	1.90	0.0161	2.84
6	1	3	2.29	0.0193	2.84
7	1.1	2	1.69	0.0108	2.37
8	1.1	2.5	2.12	0.0135	2.37
9	1.1	3	2.54	0.0162	2.37

In this study, Fig. 3 is considered as: L=10m, θ=1rad, D=1m, d=0.7m and Ld=2m. The center of the rotation is positioned at x=0 and y=0, the radius of the circle arc wave tank R is 9.7m (as shown in the Fig.2), the radius form the center of rotation to the water free surface is 10m and the length of wave tank which on the water free surface L is 10m. The mesh height considered in this study had 20 cells in the two times wave height around the water free surface and for the other regions the mesh height is bigger than that. The mesh length considered in this study is no greater than 3 times of the wave height which in the reinforced regions except the damping zone in which the wave length is greater than that. And the size of the mesh is found to be sufficiently small. A time step of T/1000 is found to be sufficiently small such that the results are independent of time step. And duration of 2T for the time ramp is found to be sufficiently big. What follows are the details and the results of the experiments.

4.1. wave generation in circle arc wave tanks

In this section the numerical results in the case of wave generation in a circle arc wave tank are compared with analytics in order to verify the accuracy of the results. And for this purpose, the wavemaker theory of Ursell et al. [10] and the 1st order Stokes' progressive waves (also the Airy waves) are considered.

All nine cases are studied in this section, which can be divided into three categories based on the wave periods. In these cases, to obtain the values of the wave profile from numerical calculations, a section away form the wavemaker and the damping zone at the end of the wave tank is considered. This section is selected between two positions distanced 1m away form the wavemaker location and 8m which in front of the damping zone in order to obtain the wave height distribution of the wave filed in the wave tank. The numerical free surface profile at the dimensionless time of t/T=25 for cases with maximum wave steepness in every category (the cases #3, #6 and #9 of table 1) are shown in Fig. 4. It is seen that the wave profile reaches a steady state in the wave tanks. And the numerical and analytical results are also compared with each other at the dimensionless time of t/T=25 in Fig. 4. As observed in the figure, the numerical results from the present model agree well with the analytical results.

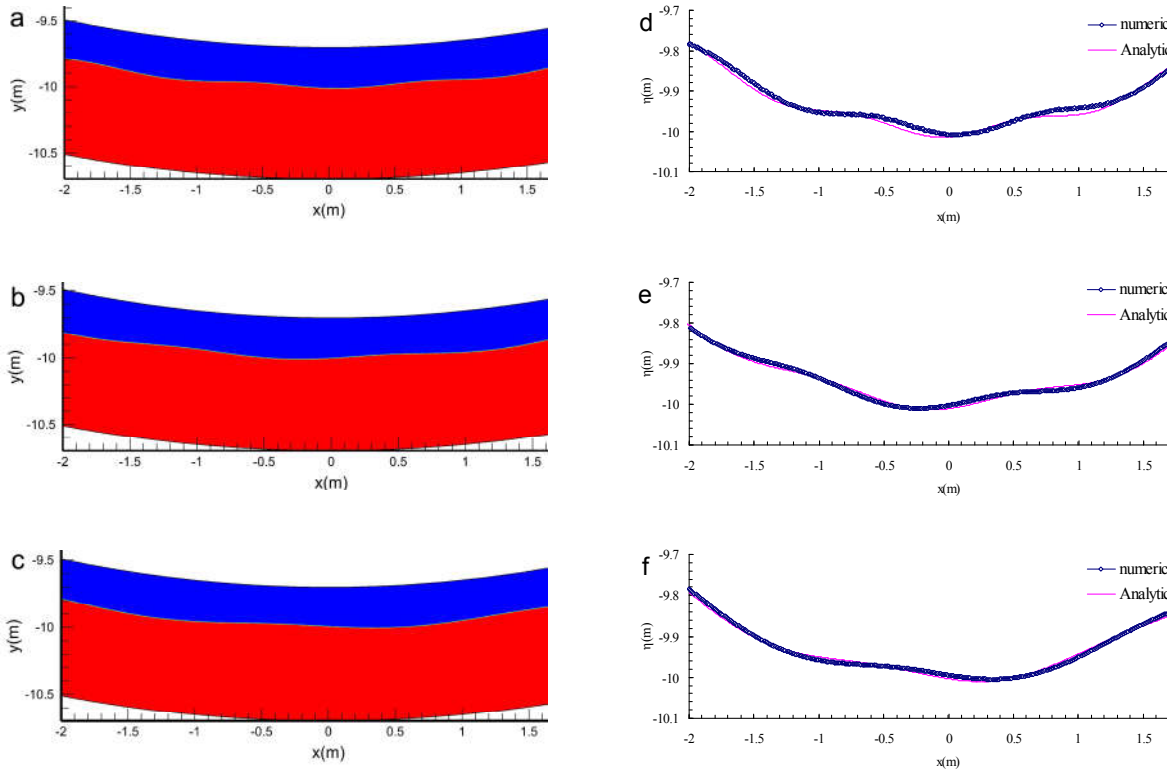

Fig. 4 Numerical free surface profile at t/T=25 for: (a) No. 3; (b) No.6; and (c) No. 9 and comparison between the numerical and analytical wave profile t/T=25 for: (d) No. 3; (e) No.6; and (f) No. 9

4.2. wave generation in straight wave tanks

In this section the numerical results in the case of wave generation in a straight wave tank are presented. In the case of straight wave tanks, the numerical results are compared with analytical results as presented in Ursell et al. [10] and the 1st order Stokes' progressive waves in order to verify the accuracy of the results.

All nine cases are studied in this section, which can be divided into three categories based on the wave periods. In these cases, to obtain the values of the wave profile from numerical calculations, a section away form the wavemaker and the damping zone is selected, too. The numerical free surface profile at the dimensionless time of t/T=25 for cases with maximum wave steepness in every category (the cases #3, #6 and #9 of table 1) are shown in Fig. 5. It is seen that the wave profile reaches a steady state in the wave tanks. And the numerical and analytical results are also compared with each other at the dimensionless time of t/T=25 in Fig. 5. As observed in the figure, the numerical results from the present model agree well with the analytical results, too.

4.3. comparison of wave profile in straight wave tanks and in circle arc wave tanks

In this section the numerical results in the case of wave generation in a circle arc wave tank and in a straight wave tank are compared with each other. And also the wavemaker theory of Ursell et al. [10] and the 1st order stokes' progressive waves are considered for compared with the results in order to verify the accuracy of the results.

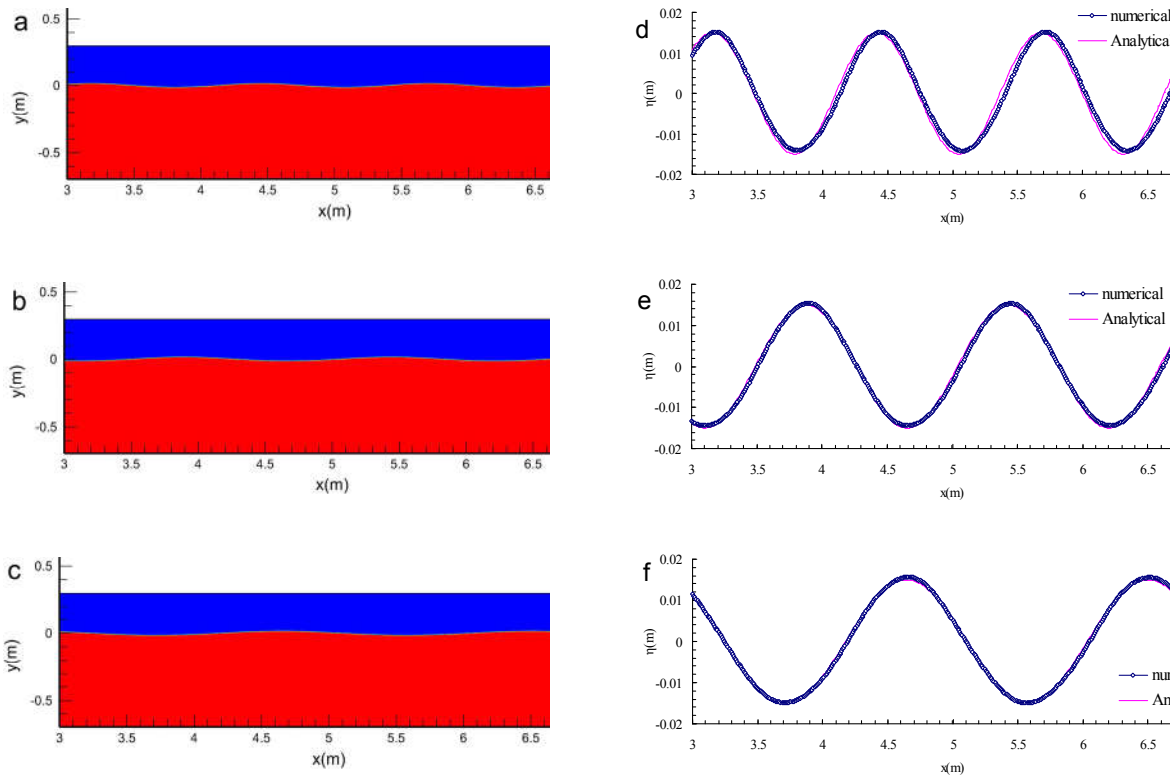

Fig. 5 Numerical free surface profile at t/T=25 for: (a) No. 3; (b)No.6; and (c) No. 9 and comparison between the numerical and analytical wave profile t/T=25 for: (d) No. 3; (e) No.6; and (f) No. 9

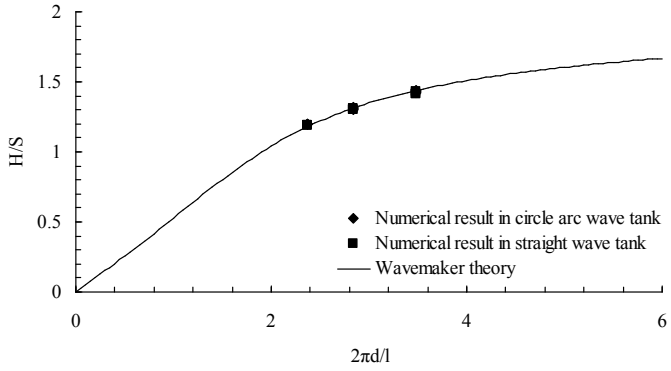

Fig. 6 Comparison between the solution of wave maker theory and numerical results

The numerical results from the present study for wave generation both in circle arc wave tanks and in straight wave tanks are compared with each other, as shown in Fig. 6. The results from the wavemaker theory are also displayed in the figure. The numerical wave height which presented in Fig. 6 is calculated by averaging the wave heights at the fixed position with the distance equal to 2m, 4m and 6m away form the wavemaker initial position. The wavelength is calculated by averaging the wave lengths taken form the free surface space distribution inside the section which between two positions distanced 2m and 6m away from the wavemaker initial position. In this study, the cases include intermediate and deep water which can be divided into three categories based on the wave periods and also the wavelength because of the wavelength which can be calculated by water depth and wave periods and all cases have the same water depth in this study, as tabulated in Table 1. As

observed in the figure, the numerical results from the present model agree well with each other both in circle arc wave tanks and in straight wave tanks. And the numerical results agree well with analytical results, too.

Figure 7 shows the time history of the numerical water free surface elevation (measured from the still water height) at 5m away from the wavemaker initial position in comparison with the analytical results. As observed in the figure, the numerical results from the present model agree well with each other and the analytical results. The slight discrepancy as displayed in figure 6 and figure 7 of the numerical results obtained from the circle arc numerical waves and the straight numerical waves can be attributed to the nonlinear effect caused by the circle arc. However, the discrepancy is insignificant which can be neglected for a circle arc wave tank with a radius of 10m.

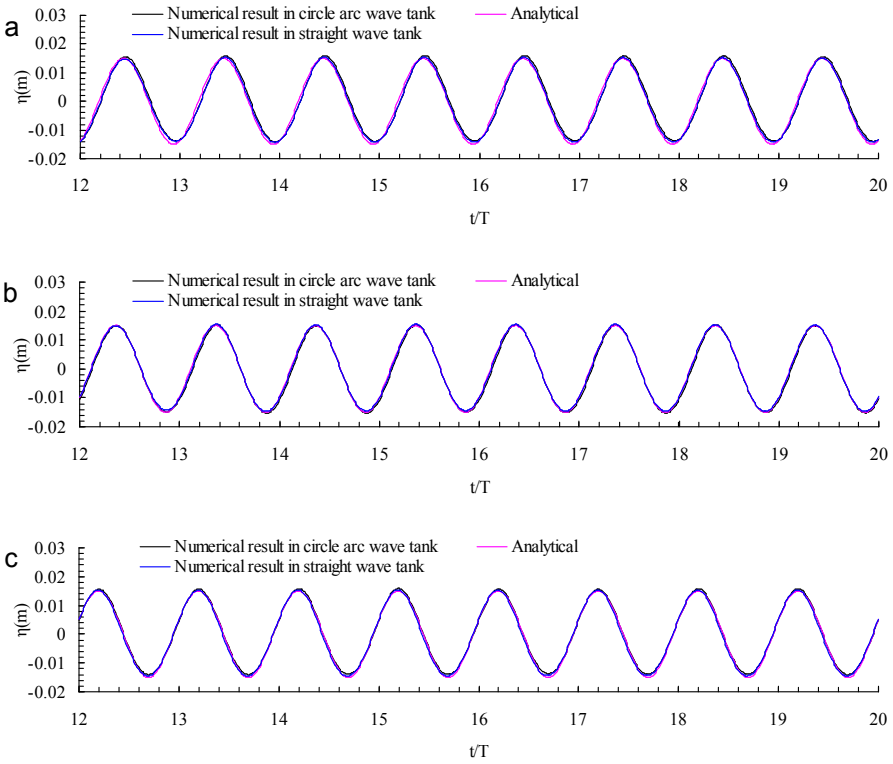

Fig. 7 Comparison between the numerical and analytical free surface elevation at x=5m for: (a) No. 3; (b) No.6 and (c) No. 9

5. Conclusion

The circle arc numerical wave tank is presented in this paper that can be used in a geotechnical centrifuge for wave generation. And the use of the circle arc numerical wave tank can minimize the error due to the radial gravity field which produced by the centrifugal acceleration. A variety of cases generated by flap-type wavemakers in intermediate and deep waters are simulated in the circle arc wave tanks and the accuracy of the results are verified by a comparison with the results of wavemaker theory and the numerical results in straight wave tanks.

The following conclusions of this study can be drawn:

(1) The wavemaker theory produced by Ursell can be used not only in the traditional straight numerical wave tanks but also in a circle arc numerical wave tanks.

(2) For both the traditional straight wave tanks and circle arc wave tanks, the numerical results agree well with each other and the theoretical results. The slight discrepancy of the numerical results between the circle arc wave tank and the traditional straight numerical wave tank may be attributed to

the nonlinear effect caused by the circle arc. And the nonlinear effect caused by the circle arc can be neglected in a circle arc wave tank with a radius equal to 10m.

References

[1] R.N. Taylor, Geotechnical centrifuge technology, Blackie Academic & professional, London, UK, 1995.
[2] H. Sekiguchi, R. Phillips, Gravity water waves in a drum centrifuge, Annuals, Disas. Prev. Res. Inst., Kyoto Univ., 33 (1990) 69-81.
[3] H. Sekiguchi, K. Kita, S. Sassa, et al., Generation of progressive fluid waves in a geo-centrifuge, Geotechnical Testing Journal 21 (1998) 95-101.
[4] S. Sassa, H. Sekiguchi, Wave-induced liquefaction of beds of sand in a centrifuge, Géotechnique 49 (1999) 621-638.
[5] S. Sassa, H. Sekiguchi, J. Miyamoto, Analysis of progressive liquefaction as a moving-boundary problem, Géotechnique 51 (2001) 847-857.
[6] S.E. Coulter, R. Phillips, simulating submarine slope instability initiation using centrifuge model testing. In: Proceeding of the 1st international symposium on Submarine Mass Movement and their Consequences, 2003, 29-36.
[7] S.E. Coulter, Seismic initiation of submarine slope failures using physical modeling in a geotechnical centrifuge, Master of Engineering Thesis: Memorial University of Newfoundland, 2008.
[8] N. Boylan, C. Gaudin, D.J. White, et al., Modelling of submarine slides in the geotechnical centrifuge, In: Proceedings of the 7th international conference Physical Modelling in Geotechnics, Zurich, 2010, 1095-1100.
[9] C.S. Gue, Submarine landslide flows simulation through centrifuge modelling, Doctor of Philosophy: Dissertation of the University of Cambridge, 2012.
[10] F. Ursell, R.G. Dean, Y.S. Yu, Forced small-amplitude water waves: a comparison of theory and experiment, Journal of Fluid Mechanics 7(1960) 33-52.
[11] J. Spinneken, C. Swan, Second-order wave maker theory using force-feedback control. Part I: A new theory for regular wave generation, Ocean Engineering 36 (2009) 539-548.
[12] H.A. Schäffer, Second-order wavemaker theory for irregular waves, Ocean Engineering 23 (1996) 47-88.
[13] X.Z. Zhao, C.H. Hu, Z.C. Sun, Numerical simulation of extreme wave generation using VOF method, Journal of hydrodynamics, ser. B 22 (2010) 466-477.
[14] N.J. Wu, T.K. Tsay, Y.Y. Chen, Generation of stable solitary waves by a piston-type wave maker, Wave Motion 51 (2014) 240-255.
[15] S. Nallayarasu, C.H. Fatt, N.J. Shankar, Estimation of incident and reflection waves in regular wave experiments, Ocean Engineering 22 (1995) 77-86.
[16] G. Dong, X.Z. Ma, M. Perlin, et al., Experimental study of long wave generation on sloping bottoms, Coastal Engineering 56 (2009) 82-89.
[17] C.W. Hirt, B.D. Nichols, Volume of fluid (VOF) method for the dynamics of free boundaries, Journal of computational physics 39 (1981) 201-225.
[18] A.N. Schofield, Cambridge geotechnical centrifuge operations. Géotechnique, 30 (1980) 227-268.
[19] H.R. Barker, Physical modelling of construction processes in the mini-drum centrifuge, Doctor of G. Ducrozet, F. Bonnefoy, D. Touzé, et al., A modified High-order Spectral method for wavemaker modeling in a numerical wave tank, European Journal of Mechanics B/Fluids 34 (2012) 19-34.
[20] M. Anbarsooz, M. Passandidedh- Fard, M. Moghiman, Fully nonlinear viscous wave generation in numerical wave tanks, Ocean Engineering 59 (2013) 73-85.
[21] I. Gyongy, T. Bruce, I. Bryden, Numerical analysis of force-feedback control in a circular tank, Applied Ocean Research 47 (2014) 329-343.

[22] X.Z. Zhao, C.H. Hu, Z.C. Sun, S.X. Liang, Validation of the initialization of a numerical wave flume using a time ramp, Fluid Dynamics Research 42 (2010) 045504.
[23] P. Lin, P.L.F. Liu, Discussion of "vertical variation of the flow across the surf zone" [coast. Eng. 45 (2002) 169-198], Coastal Engineering 50 (2004) 161-164.
[24] Z. Hafsia, M.B. Hadj, H. Lamloumi, et al., Internal inlet for wave generation and absorption treatment, Coastal Engineering 56 (2009), 951-959.